ORIGINAL ARTICLE

Finite Element Analysis of Percutaneous Anterograde and Retrograde Screws in the Treatment of Superior Rami Pubis Fracture

Hui Lu[1,2,3] · Shuo Han[1,2] · Zheng Lian[1,2] · Rong Liu[3,4] · Xuexiao Ma[1]

Abstract

Purpose This study aims to evaluate the biomechanical characteristics of percutaneous antegrade and retrograde screws in treating superior pubic rami fractures in zone II, employing finite element analysis. It provides a theoretical basis for the treatment of the superior rami of pubis zone II fracture.

Methods The software of Mimics and 3-Matic were utilized for reconstructing a fracture model of the superior pubic rami in zone II. Percutaneous screw implantation was simulated for treatment. Material properties were assigned using Mimics, and Ansys software was employed to simulate forces on the S1 vertebral endplate under a 500 N load in a standing posture. Mechanical stability was assessed by comparing these simulations.

Results (1) Displacement and stress variations in the pubic bone and screws were consistent across the model and on the fracture site, whether the fracture was in zone I or zone II. However, in zone III, the displacement and stress experienced by the screws were markedly higher than those in zones I and II. (2) When employing an antegrade screw to simulate treatment of a superior pubic rami fracture in zone II, the maximum displacement and stress recorded were 0.88 mm and 15.53 MPa, respectively. Conversely, the use of a retrograde screw for treating a superior pubic rami fracture yielded a maximum displacement of 0.59 mm and stress of 5.51 MPa.

Conclusion The biomechanical analysis suggests that for zone II superior pubic rami fractures, where the fracture line is no more than 70 mm from the insertion point (encompassing zones I and II fractures), the use of retrograde screw implantation is preferable.

Keywords Transcutaneous Anterograde Screw · Percutaneous Retrograde Screw · Fracture of Superior rami Pubis · Finite Element Analysis · Pelvic Fractures

Hui Lu and Shuo Han contributed equally to this work and shared the first authors. Rong Liu and Xuexiao Ma shared the corresponding authors.

✉ Rong Liu
dr_liurong@whu.edu.cn

✉ Xuexiao Ma
maxuexiaospinal@163.com

1 Department of Spinal Surgery, The Affiliated Hospital of Qingdao University, Qingdao, China

2 Department of Medicine, Qingdao University, Qingdao, China

3 Institute of Medical Innovation and Transformation, Puren Hospital affiliated to Wuhan University of Science and Technology, Wuhan, China

4 Department of Orthopedics, Puren Hospital affiliated to Wuhan University of Science and Technology, Wuhan, China

1 Introduction

Pelvic fractures constitute approximately 4.2% of all body fractures [1], predominantly occurring due to vehicular accidents and falls from significant heights. Classified as a critical orthopedic injury [2, 3], these fractures have mortality rates ranging between 20% and 60% [4–6], with certain reports indicating rates up to 70% [7]. Stable pelvic fractures typically receive conservative treatment, whereas unstable fractures, especially those involving the posterior ring, often result in poor clinical outcomes and a high complication rate. Reduction and internal fixation are considered the gold standard for these injuries [8]. The focus of pelvic fracture treatment has traditionally been on the posterior pelvic ring. However, recent biomechanical research has shifted this focus, emphasizing the importance of restoring the stability of both the posterior and anterior pelvic ring structures

[9]. The stability of the anterior pelvic ring contributes 40% to the overall pelvic stability [10]. Fractures of the pubic branch, a common type of anterior pelvic ring injury, have significant biomechanical implications. Stabilizing these fractures not only reduces stress on the posterior pelvic ring fixation system but also enhances the stability of the entire pelvic ring [11].

Currently, methods for fixing anterior pelvic ring injuries primarily encompass anterior subcutaneous fixation, external fixation, plate internal fixation, and percutaneous screw internal fixation [12]. Percutaneous screw fixation, known for being minimally invasive, offers benefits such as reduced soft tissue damage and decreased intraoperative blood loss. In recent years, the accumulation of surgical expertise and advancements in intraoperative fluoroscopy have facilitated its growing application in the treatment of anterior pelvic ring fractures [13–15]. ROUTT et al. [16], as early as 1995, pioneered the use of percutaneous hollow screws for pubic rami fractures. This innovation provided a novel approach for pelvic fracture treatment, leveraging computer-aided navigation technology [17].

According to Nakatani's zoning criteria for pubic rami fractures [18], these fractures are categorized into zone III. During clinical observations, the prevalence of pubic rami fractures in zone II has been noted, prompting further investigation. This study aims to analyze the biomechanical stress in zones I, II, and III of the pubic rami to elucidate the propensity for fractures in zone II. Additionally, screw implantation techniques can be classified into antegrade and retrograde screw fixation [19]. Currently, there is no consensus on the superior method. This research investigates the biomechanical properties of percutaneous antegrade and retrograde screws in treating zone II superior pubic branch fractures using finite element analysis. The findings are intended to provide a theoretical foundation for selecting the direction of screw implantation in clinical treatment of these fractures.

2 Data and Methods

2.1 Objects

A healthy male volunteer, age 27, height 170 cm, weight 60 kg, was selected as the observation object.

Inclusion criteria: (1) The volunteers could follow the doctor's advice and complete relevant imaging examinations to exclude bone destruction such as tumor, deformity and pathological fracture; (2) Pelvic data obtained by CT scan; (3) Sign the relevant informed consent form.

Main instruments: 64-slice spiral CT (Siemens, Germany), Mimics 20.0 (Materialise, Belgium), 3-Matic 12.0 (Materialise, Belgium), Ansys 19.2 (Ansys, USA).

3 Methods

3.1 CT Data Acquisition

A 64-slice spiral CT scanner was employed to conduct pelvic scans on volunteers. The scanning parameters included a voltage of 140 kV and a current of 200 mA, with a slice thickness of 0.625 mm. The CT data were extracted in the DICOM format with a resolution of 512×512 pixels [20].

3.2 Establishment of Three-Dimensional Pelvis Model

CT data from volunteers were imported into Mimics 20.0 software for three-dimensional reconstruction of the pelvis. This process involved establishing a geometric model of the entire pelvis. Subsequently, the data were imported into 3-Matic 12.0 software in STL format. Utilizing tools provided by the software, such as mesh diagnosis and surface parameter fitting, the surface mesh and body mesh of the pelvis were segmented [21]. This approach facilitated the generation of a three-dimensional solid pelvis model.

3.3 Finite Element Model Establishment

The three-dimensional pelvis model was imported into Ansys 19.2 software for the establishment of a complete finite element model, with material properties being assigned in this process. Material assignment was carried out using Mimics 20.0 software. This study assumes that the mechanical properties of bone and internal fixation materials are homogeneous, continuous, and isotropic. The weighted balance method was employed to allocate material properties to each bone block and ligament. Specific material parameters are outlined in Table 1 [22–25]. Verification of anatomical morphological differences [26, 27] : The distance of each landmark point of the three-dimensional pelvic model and the finite element model was measured and compared.

3.4 Establishment of Finite Element Model of Anterograde and Retrograde Percutaneous Screw Simulation for the Treatment of Superior Rami of Pubis Zone II Fracture

According to the zoning criteria for fractures of the superior rami of the pubis proposed by Nakatani [18], these fractures

Table 1 Finite element model and properties of internal fixation materials

Material	Elastic modulus, E(MPa)	Poisson ratio, μ	Stiffness Coefficient
Cortical bone	17,000	0.30	-
Cancellous bone	132	0.20	-
Sacral bone	6140	0.30	-
Femur	18,200	0.38	-
Cartilago articularis	54	0.40	-
Acetabulum cartilage	12	0.42	-
Symphysis pubis	5	0.45	-
Sacrospinous ligament	-	-	1400
Ligamentum sacrotuberale	-	-	1500
Superior pubic ligament	-	-	500
Arcuate pubic ligament	-	-	500
Screw (titanium alloy)	114,000	0.30	-

are categorized into three types, including zone I、zone II and zone III. This classification system defines zone I as the zone extending from the pubis to the medial margin of the obturator foramen, zone II as the zone from the medial to the lateral margin of the obturator foramen, and zone III as the zone beyond the lateral margin of the obturator foramen [28, 29]. Refer to Fig. 1 for a detailed illustration.

The insertion point (M point) for the retrograde screw was determined to be (7.5 ± 0.5) mm below the midpoint of the pubic ridge [30]. A long cylindrical simulated screw was implanted into the left superior pubic branch, ensuring that the screw did not penetrate the cancellous bone during the simulation. The path of the screw traversed from below the midpoint of the left pubic ridge, through the left iliac cortical bone, along the pubic channel. The distance (MN), representing the maximum length of the entire nail path, was 127 mm. Concurrently, the point where the screw traverses the left cortical bone of the iliac crest along the pubic channel was designated as the entry point (N point) for the anterograde screw. According to clinical experience, screw length is generally 30 mm from the point of entry to beyond the fracture line, therefore, screw length from the point of entry to beyond the fracture line 0–30 mm, the longer the screw length can provide better stability. However, previous studies have shown that the fracture risk of overly long (length > 100 mm) and excessively thin (diameter < 6.5 mm) screws is significantly increased [31]. Therefore, in this study, the screw diameter was set at 6.5 mm, and the length of the screw was adjusted based on specific requirements, with a maximum length not exceeding 110 mm.

This study assumes the implantation of both anterograde and retrograde screws into the left superior branch of the pubis, utilizing the same nail path for both methods. The midpoint A of the distance MN was selected, indicating the occurrence of a fracture in the superior rami of the pubis in zone II. The distances MA and NA were measured to be 65 mm each. The screw length was established at 95 mm, provided it crossed the fracture line by more than 30 mm. Accordingly, the lengths of both the anterograde screw (NC) and the retrograde screw (MB) were set to 95 mm,

Fig. 1 Classification zone of Nakatani suprapubic branch fracture and simulation of three types of suprapubic branch fracture. (A) Regional division of Nakatani suprapubic branch fracture; (B)(C)(D) Simulation of the fracture of the superior rami of the pubis in zones I, II, and III (The red arrow indicates the site of the simulated fracture)
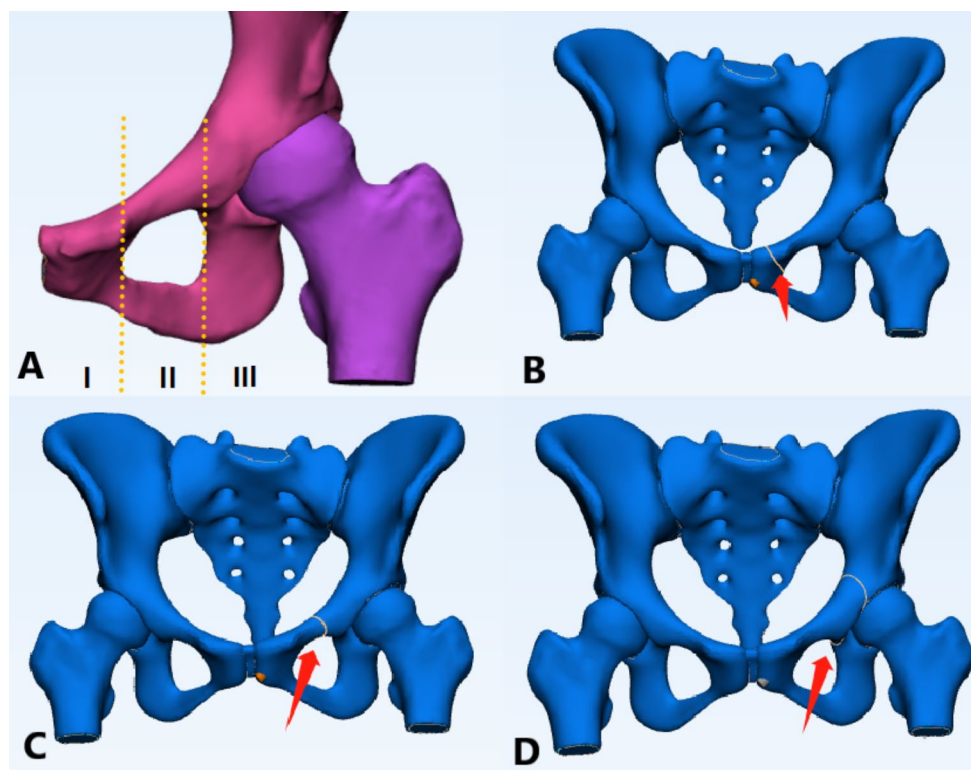
Table 2 Marking points and explanation of the model of percutaneous anterograde and retrograde screw implantation for superior ramus pubis fractures

Marking points	Explanation
Point M	Entry point of percutaneous retrograde screw implantation
Point N	Entry point of percutaneous anterograde screw implantation
Point A	The median point of MN, the distance between MA and NA is 65 mm
Point B	Point A is retrogradely extended by 30 mm, the length of MB
Point C	Point A is retrogradely extended by 30 mm, the length of NC
MN	Maximum length of the entire nail path, 127 mm
MB	Length of percutaneous retrograde screw, 95 mm
NC	Length of transcutaneous screw, 95 mm

as detailed in Table 2. The 3-Matic 12.0 software was used to create a fracture line perpendicular to the screw channel at point A, simulating the fracture of the left superior pubic branch in zone II treated with both anterograde and retrograde screws. Refer to Fig. 2 for a visual representation.

Following the outlined procedures, a finite element model was developed to simulate the use of both anterograde and retrograde percutaneous screws in the treatment of zone II superior pubic branch fractures. Material properties were assigned accordingly. Binding contacts were established between the sacrum, iliac crest, pubis, and the screws, as well as between the screws and the cortical and cancellous bones of the iliac crest. The S1 vertebral endplate was designated as the loading surface, where a 500 N load was applied vertically downwards. The cross-section of the lower end of both femurs was selected as the fixed surface, constraining movement in all six directions. This setup aimed to simulate the stress state of the human body in a standing posture.

3.5 Main Observation Indicators

(1) Structure of the pelvic three-dimensional finite element model; (2) Analysis of model validity verification results; (3) Displacement and stress distribution when 500 N load is applied to the end plate of S1 vertebral body standing position; (4) The displacement and stress distribution after fracture of the superior rami of pubis in three zones were compared by finite element analysis; (5) Analysis of displacement and stress in zone II of the superior rami of the pubis with transcutaneous anterograde and retrograde screw simulations.

4 Results

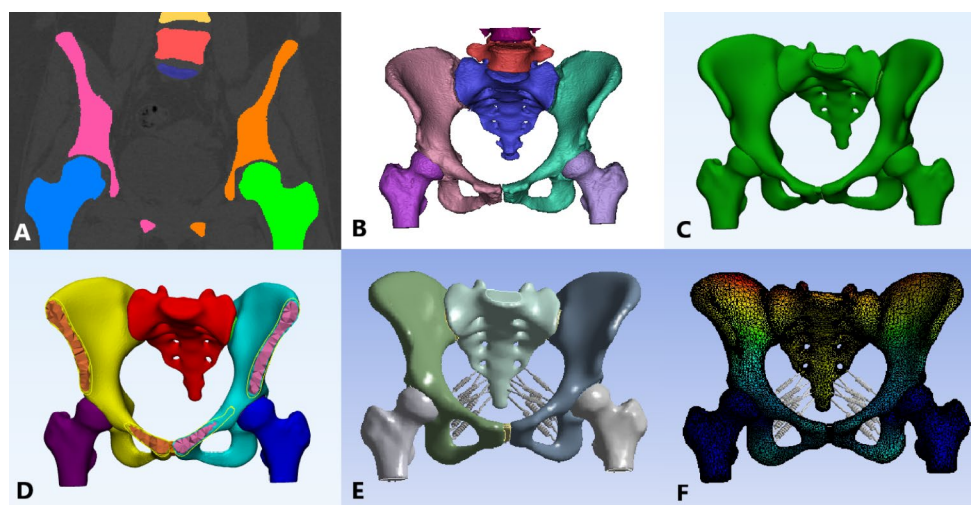### 4.1 Pelvic Three-Dimensional Finite Element Model Structure

A three-dimensional finite element model of the pelvis was developed, simulating the three-dimensional structures of various components including cortical bone, cancellous bone, sacrum, femur, sacroiliac articular cartilage, acetabular cartilage, symphysis pubis cartilage, sacrospinous
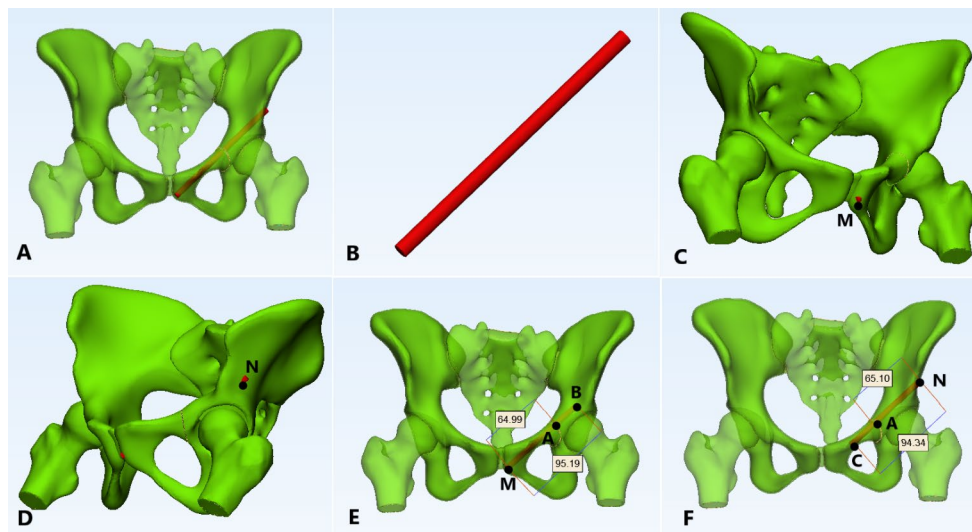
Fig. 2 Establishment process of 3D model of screw simulation treatment of suprapubic branch fracture.(**A**-**B**) Using screws to simulate the treatment of the fracture of the superior rami of the pubis. Long red cylinders were used to simulate screws. The explanation of each mark is shown in Table 2. (**C**) Entry point M of the retrograde screw; (**D**) Entry point N of the anterograde screw; (**E**) Retrograde screw simulation treatment of superior pubic branch fracture, MA is the distance from the entry point of the retrograde screw to the fracture line 65 mm, MB is the length of the retrograde screw 95 mm; (**F**) Anterograde screw simulation treatment of superior pubic branch fracture, NA is the distance from the entry point of the retrograde screw to the fracture line 65 mm, NC is the length of the retrograde screw 95 mm

Fig. 3 Three-dimensional reconstruction of pelvis and finite element model. (**A**) pelvic threshold extraction; (**B**) Preliminary three-dimensional pelvis model; (**C**) Surface grid division; (**D**) Body grid division; (**E**) Preliminary finite element model of pelvis; (**F**) Finite element model of pelvis after assignment and loading

Table 3 Comparison of the distance between three-dimensional pelvic model (TDM) and the finite element model (FEM) (mm)

Model	①	②	③	④	⑤	⑥	⑦	⑧	⑨
TDM	145.25	98.78	175.36	110.23	54.30	57.86	116.13	117.34	29.46
FEM	146.33	98.94	177.21	112.24	53.27	58.14	116.49	117.68	28.53

ligament, sacrotuberous ligament, superior pubic ligament, and arcuate ligament. Post non-uniform assembly node sharing and standardized mesh processing, the model comprised 254,022 surface meshes, 992,813 individual meshes, 43,018 nodes, and 89,813 units. Specifically, the sacrum consisted of 6,811 nodes and 13,676 units; the left iliac cortical bone had 9,191 nodes and 18,382 units, while its cancellous bone had 4,141 nodes and 8,282 units. The right iliac cortical bone comprised 9,182 nodes and 18,364 units, and its cancellous bone contained 4,189 nodes and 8,378 units. The left femur was represented with 2,782 nodes and 5,560 units; the right femur had 2,774 nodes and 5,544 units. Refer to Fig. 3 for a detailed illustration.

4.2 Analysis of Model Validity Verification Results

Table 3 presents a comparison of the distances between landmarks in both the three-dimensional pelvic model and the finite element model. The observed discrepancies in distances between corresponding landmarks in the two models are minimal. This consistency indicates the effectiveness of the finite element model.

4.3 Pelvic Displacement and Stress Distribution in Standing Position

In a standing position, the pelvis exhibited a maximum displacement of 2.4212 mm and a peak stress of 27.614 MPa. The sacrum experienced a maximum displacement of 2.3519 mm and a stress of 13.032 MPa. For the left iliac crest, the maximum displacement was recorded at 2.27 mm

and the stress at 22.619 MPa. The right iliac bone showed a maximum displacement of 2.4213 mm and a stress of 24.614 MPa. Regarding the femurs, the left femur had a maximum displacement of 0.1843 mm and a stress of 20.983 MPa, while the right femur displayed a displacement of 0.1954 mm and a stress of 23.386 MPa. These findings are illustrated in Figs. 4 and 5, and Fig. 6.

4.4 The Finite Element Analysis of the Treatment of Different Superior Pubic Branch Fractures

Table 4 presents a comparative analysis of the finite element analysis results for three types of superior pubic branch fractures. As indicated by the data in the table, the displacement and stress variations in the pubic bone and percutaneous hollow screws, both in the overall model and on the fracture side, were similar when the fracture occurred in zone I and zone II. Notably, the displacement and stress in the screws located in zone III were significantly higher than those in zones I and II. This data is further illustrated in Figs. 7 and 8, and Fig. 9.

4.5 Finite Element Analysis of Percutaneous Anterograde and Retrograde Screws for the Treatment of Superior Rami Pubis Fracture in Zone II

When an anterograde screw was utilized to simulate the treatment of superior rami of the pubis in zone II, the maximum displacements observed were 2.40 mm for the pelvis, 2.35 mm for the left pubic bone, and 0.88 mm for the screw. Correspondingly, the maximum stresses were 26.41 MPa

Fig. 4 Three views of pelvic displacement and stress distribution in standing position. Three views of pelvic displacement distribution in (**A**)-(**C**) Standing position, (**A**) Frontal view; (**B**) Side view; (**C**) Top view; (**D**)-(**F**) Three views of pelvic stress distribution in standing position, (**D**) Frontal view; (**E**) Side view; (**F**) Top view
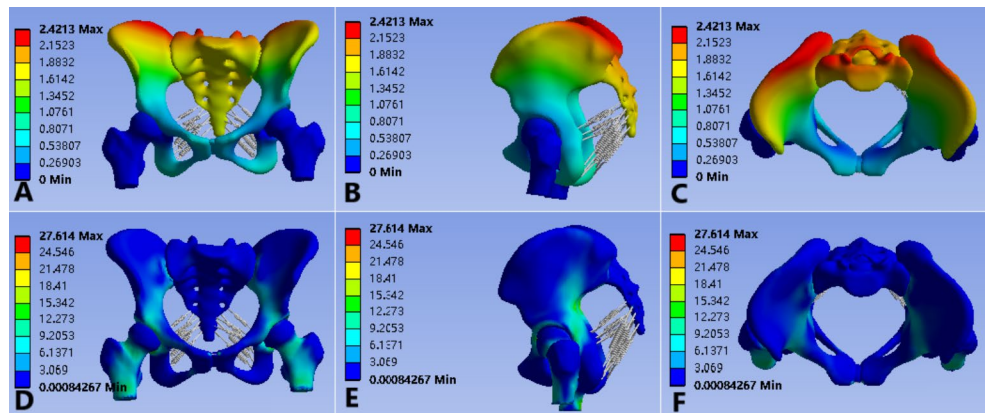

Fig. 5 Displacement distribution in standing position. (**A**) Pelvis; (**B**) Sacrum; (**C**) Left iliac crest; (**D**) Right iliac bone; (**E**) Left femur; (**F**) Right femur
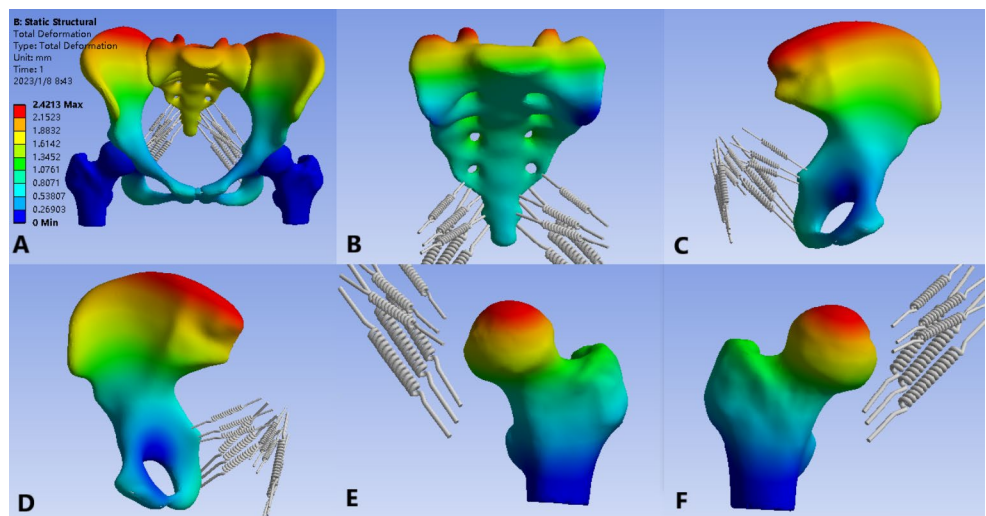
Fig. 6 Stress distribution in standing position. (**A**) Pelvis; (**B**) Sacrum; (**C**) Left iliac crest; (**D**) Right iliac bone; (**E**) Left femur; (**F**) Right femur
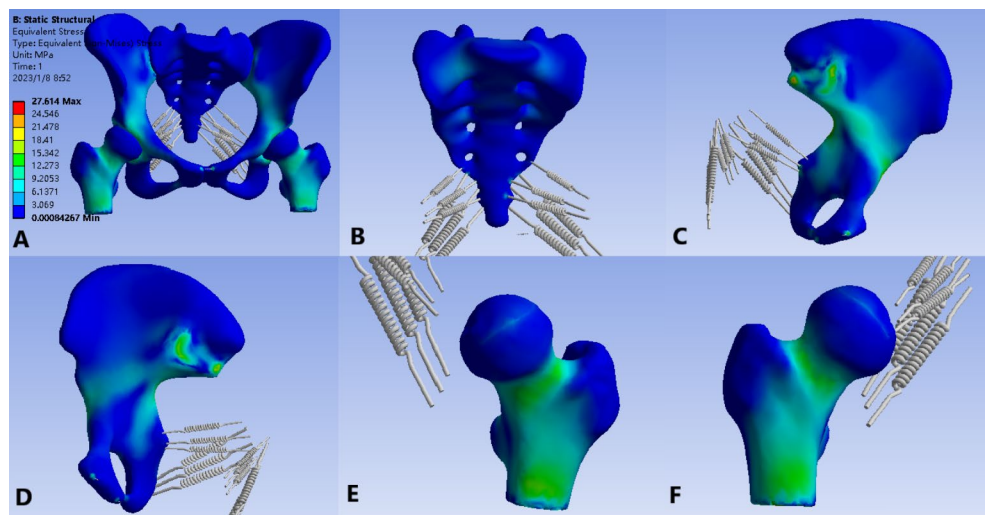
Fig. 7 Effect of superior rami pubis fracture on pelvic displacement and stress distribution. (**A**) Zone I fracture - displacement distribution; (**B**) Zone II fracture - displacement distribution; (**C**) Zone III fracture - displacement distribution; (**D**) Zone I fracture - stress distribution; (**E**) Zone II fracture - stress distribution; (**F**) Zone III fracture - stress distribution
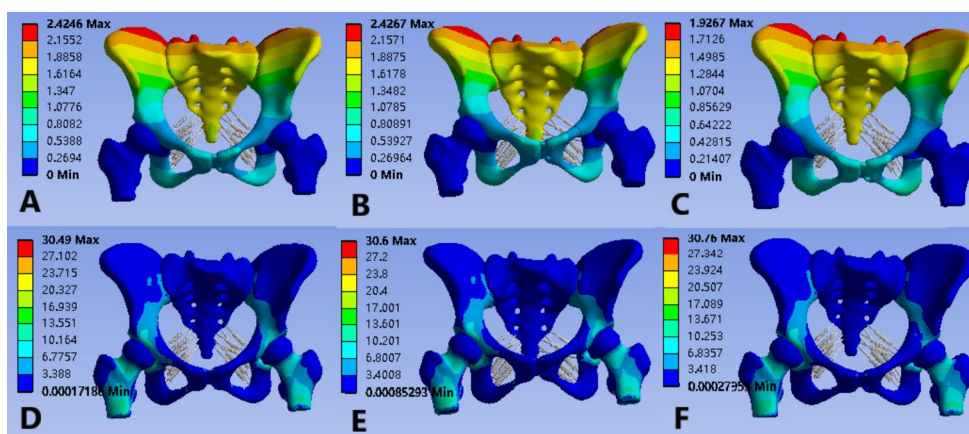
Fig. 8 Effects of superior rami pubis fracture on the displacement and stress distribution of the pubic bone on the fractured side. (**A**) Zone I fracture - displacement distribution; (**B**) Zone II fracture - displacement distribution; (**C**) Zone III fracture - displacement distribution; (**D**) Zone I fracture - stress distribution; (**E**) Zone II fracture - stress distribution; (**F**) Zone III fracture - stress distribution
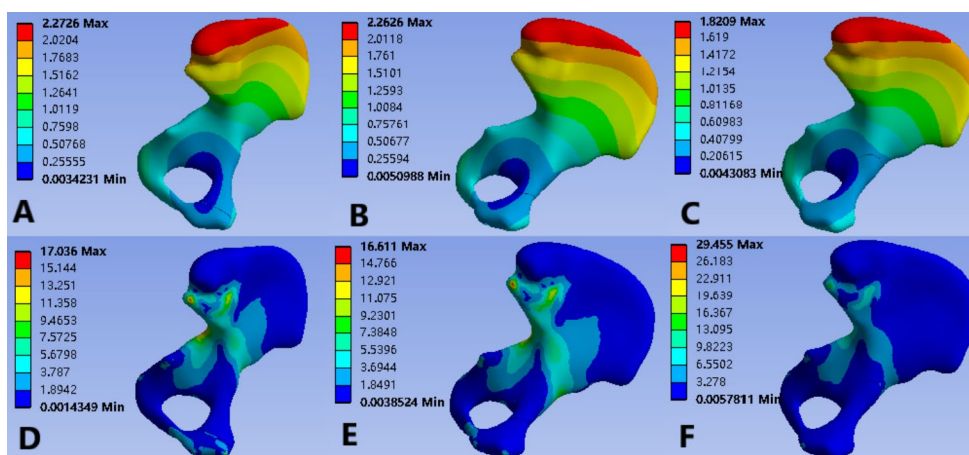
Fig. 9 Effect of superior rami pubis fracture on screw displacement and stress distribution. (**A**) Zone I fracture - displacement distribution; (**B**) Zone II fracture - displacement distribution; (**C**) Zone III fracture - displacement distribution; (**D**) Zone I fracture - stress distribution; (**E**) Zone II fracture - stress distribution; (**F**) Zone III fracture - stress distribution
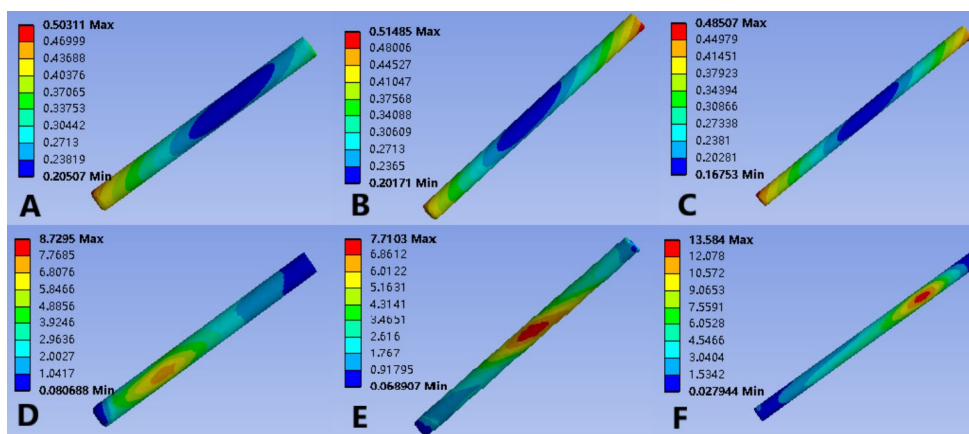

for the pelvis, 17.96 MPa for the left pubic bone, and 15.53 MPa for the screw, as depicted in Fig. 10.

In the simulation involving a retrograde screw for treating the superior branch of pubis fracture, the maximum displacements recorded were 2.40 mm for the pelvis, 2.35 mm for the left pubic bone, and 0.59 mm for the screw. The highest stress values measured were 33.13 MPa for the pelvis, 18.29 MPa for the left pubic bone, and 5.51 MPa for the screw, as shown in Fig. 11.

4.6 Discussion

Figures 4, 5 and 6 reveal that the acetabulum, symphysis pubis, and sacroiliac joints of the pelvis endure substantially higher stress compared to other zones. As can be seen from Table 4, the entire model was subjected to about 30 MPa of stress when the suprapubic branch fractures occurred in zone I, zone II and zone III. This is because the three models were loaded with the same force. Although the three types of suprapubic branch fractures occurred, their impact on the

Fig. 10 Displacement and stress distribution of the superior rami of the pubis fracture treated with a anterograde screw simulation. (**A**) Pelvic displacement distribution; (**B**) Displacement map of left pubis; (**C**) Screw displacement distribution diagram; (**D**) Pelvic stress distribution map; (**E**) Stress distribution map of left pubic bone; (F) Screw stress distribution diagram
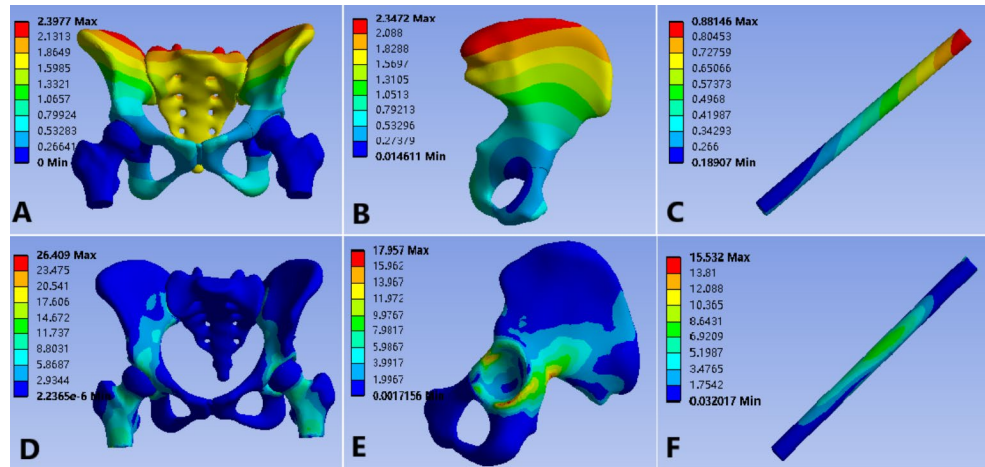
Fig. 11 Displacement and stress distribution of the superior ramus fracture treated with retrograde screw simulation. (A) Pelvic displacement distribution; (B) Displacement map of left pubis; (C) Screw displacement distribution diagram; (D) Pelvic stress distribution map; (E) Stress distribution map of left pubic bone; (F) Screw stress distribution diagram
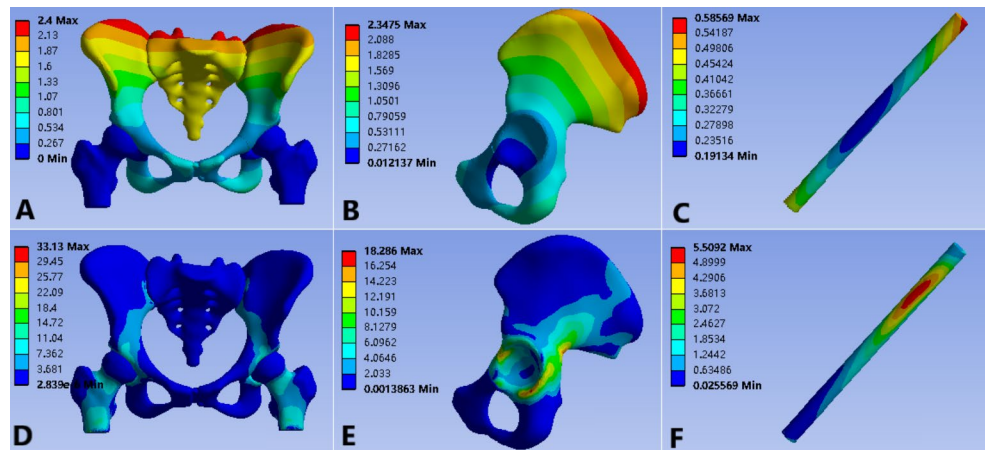
entire pelvis was small. The stress on the pubic bone on the fracture side was 17.04 MPa, 16.61 MPa, and 13.58 MPa in zones I, II, and III suprapubic rami fractures, respectively, because the stress on the suprapubic rami fracture in zone III was borne by the screw. The stresses of the screws in the fractures of the I, II and III suprapubic rami were 8.73 MPa, 7.71 MPa and 29.46 MPa, when a fracture occurs in the superior rami of the pubis in zone III, both the displacement and stress experienced by the screws are significantly greater than those in zones I and II. This observation led to further analysis, suggesting that the fracture site in zone III of the superior rami of the pubis is proximal to the pelvis's primary stress-bearing zone. As depicted in Fig. 6, the stress sustained by the pelvis and acetabulum is notably higher than in other zones of the pelvis. This finding may explain the elevated stress on the screw during fractures of the superior rami of the pubis in zone III.

Figures 10 and 11 indicate that in the treatment of superior pubic branch fractures in zone II using both anterograde and retrograde screws, the displacement differences between the pelvis and the left pubic bone were negligible. Specifically, with the anterograde screw, the maximum displacement of the pelvis was 2.40 mm, that of the left pubic bone was

2.35 mm, and the screw was 0.88 mm; with the retrograde screw, these values were 2.40 mm, 2.35 mm, and 0.59 mm, respectively. The variations were primarily observed in the screws, with anterograde screws exhibiting greater deformation. The stress on the anterograde screw (15.53 MPa) exceeded that on the retrograde screw (5.51 MPa), suggesting a higher likelihood of breakage in the anterograde screw. When comparing the total stress on the pelvis and the left pubic bone, there was no significant difference between the anterograde and retrograde screw applications (anterograde: maximum pelvic stress was 26.41 MPa, left pubic bone stress was 17.96 MPa; retrograde: pelvic stress was 33.13 MPa, left pubic bone stress was 18.29 MPa). However, under retrograde screw treatment, the pelvis experienced greater stress, indicating that the stress from the retrograde screw was transferred to the pelvis, thereby reducing the stress on the screw. Consequently, from a biomechanical perspective, retrograde screw implantation appears to be more effective for treating zone II superior pubic branch fractures.

During the screw implantation process, it was observed that the displacement and stress exerted on the anterograde screw were higher compared to the retrograde screw. This was attributed to the anterograde screw having to traverse

the pelvis's main stress-bearing zone, specifically the upper part of the acetabular zone, which increases the stress on the screw and consequently heightens the risk of screw breakage. Therefore, the stress experienced by the anterograde screw exceeds that of the retrograde screw. These findings offer insights into the optimal direction for screw placement. In cases where the superior pubic branch fracture is proximal to zone III, selecting a anterograde screw placement is advisable, as retrograde screw placement would necessitate a longer screw. Conversely, if the superior pubic branch fracture occurs in zone III, there is often an associated acetabular fracture due to the increased stress in this zone. In such scenarios, screw fixation alone may be insufficient, necessitating simultaneous plate fixation. For fractures of the superior rami of the pubis closer to zone I, retrograde screw implantation can be chosen to achieve satisfactory outcomes.

Of course, in clinical work, we have found that many patients with suprapubic rami fractures in zone I and II are treated with percutaneous screws, and there are also many patients with suprapubic rami fractures in zone III. However, because suprapubic rami fractures in zone III are often combined with acetabular fractures, percutaneous screws are generally not used for treatment alone. More often the acetabulum is fixed with plates and screws. Therefore, percutaneous screws are more commonly used in the treatment of patients with fractures of the superior rami of the pubis in zones I and II. For zone I suprapubic branch fractures, percutaneous retrograde screw treatment is preferred because the retrograde entry point is closer to the fracture line. If the fracture line is closer to zone I, percutaneous retrograde screws are used to treat the superior rami fractures in zone II. If the fracture line is closer to zone III, percutaneous anterograde screws are used. This study is also consistent with the clinical application. According to the findings of this study, when the distance between the fracture line and the entry point is not more than 70 mm for the suprapubic branch fractures in zone II (the suprapubic branch fractures in zone I and II), retrograde screw implantation is recommended.

This study acknowledges certain limitations [32]: (1) The replication of the pelvic structure was not exhaustive; the simulation included only the bony framework, major ligaments, and cartilages of the pelvis. In reality, pelvic fractures often result from high-energy impacts such as vehicular accidents and falls from significant heights [2, 3]. This suggests that the stability of the pelvis is robust and heavily relies on the support of these auxiliary ligaments. (2) The simulation did not encompass the full physiological state of the human body, focusing only on the standing posture. Future efforts will concentrate on enhancing our technology, refining the model-building process, and achieving a more accurate simulation of the human body's

physiological state. This will aim to provide a more robust theoretical foundation for both researchers and clinicians.

In summary, biomechanical considerations suggest that for superior pubic rami fractures in zone II, when the distance between the fracture line and the insertion point is no more than 70 mm (as in fractures of zones I and II), retrograde screw implantation is recommended. However, it is crucial to note that the selection of specific surgical methods should be aligned with the actual clinical scenario. Factors such as the complexity of the surgery and the surgeon's experience can significantly influence the outcome of the procedure.

Declarations

References

1. Zhang Yingze. (2011). Some suggestions on the treatment of pelvic fracture. *Chinese Journal of Orthopedics*, *31*(11), 1183–1184.
2. Hung, C. C., Wu, J. L., Li, Y. T., Cheng, Y. W., Wu, C. C., Shen, H. C., & Yeh, T. T. (2018). Minimally invasive treatment for

anterior pelvic ring injuries with modified pedicle screw-rod fixation: A retrospective study. *J Orthop Surg Res*, 13, 238.

3. Li, L., Lu, J., Yang, L., Zhang, K., Jin, J., Sun, G., Wang, X., & Jiang, Q. (2019). Stability evaluation of anterior external fixation in patient with unstable pelvic ring fracture: A finite element analysis. *Annals of Translational Medicine*, 7, 303.

4. Starr, A. J., Griffin, D. R., Reinert, C. M., Frawley, W. H., Walker, J., Whitlock, S. N., Borer, D. S., Rao, A. V., & Jones, A. L. (2002). Pelvic ring disruptions: Prediction of associated injuries, transfusion requirement, pelvic arteriography, complications, and mortality. *Journal of Orthopaedic Trauma*, 16(8), 553–561.

5. Cothren, C. C., Osborn, P. M., Moore, E. E., Morgan, S. J., Johnson, J. L., & Smith, W. R. (2007). Preperitonal pelvic packing for hemodynamically unstable pelvic fractures: a paradigm shift. J Trauma. ;62(4):834-9; discussion 839–842.

6. Eastridge, B. J., Starr, A., Minei, J. P., O'Keefe, G. E., & Scalea, T. M. (2002). The importance of fracture pattern in guiding therapeutic decision-making in patients with hemorrhagic shock and pelvic ring disruptions. *Journal of Trauma*, 53(3), 446–450. discussion 450–451.

7. Dente, C. J., Feliciano, D. V., Rozycki, G. S., Wyrzykowski, A. D., Nicholas, J. M., Salomone, J. P., & Ingram, W. L. (2005). The outcome of open pelvic fractures in the modern era. *American Journal of Surgery*, 190(6), 830–835.

8. Matta, J. M., Mehne, D. K., & Roffi, R. (1986). Fractures of the acetabulum. Early results of a prospective study. *Clinical Orthopaedics and Related Research*. ;(205):241–250.

9. Marecek, G. S., & Scolaro, J. A. (2018). Anterior Pelvic Ring: Introduction to evaluation and management. *Journal of Orthopaedic Trauma*, 32(Suppl 6), S1–S3.

10. Newhouse, K. E., el-Khoury, G. Y., & Buckwalter, J. A. (1992). Occult sacral fractures in osteopenic patients. *Journal of Bone and Joint Surgery. American Volume*, 74(10), 1472–1477.

11. Lei, J., Zhang, Y., Wu, G., Wang, Z., & Cai, X. (2015). The influence of pelvic Ramus fracture on the Stability of fixed pelvic complex fracture. *Computational and Mathematical Methods in Medicine*, 2015, 790575.

12. Stevenson, A. J., Swartman, B., & Bucknill, A. T. (2016). Percutaneous internal fixation of pelvic fractures. *German Version] Unfallchirurg*, 119, 825–834.

13. Quercetti, N., Horne, B., DiPaolo, Z., & Prayson, M. J. (2017). Gun barrel view of the anterior pelvic ring for percutaneous anterior column or superior pubic ramus screw placement. *European Journal of Orthopaedic Surgery & Traumatology*, 27, 695–704.

14. Liu, H. S., Duan, S. J., Liu, S. D., Jia, F. S., Zhu, L. M., & Liu, M. C. (2018). Robot-assisted percutaneous screw placement combined with pelvic internal fixator for minimally invasive treatment of unstable pelvic ring fractures. *Int J Med Robot*, 14, e1927.

15. Banaszek, D., Starr, A. J., & Lefaivre, K. A. (2019). Technical considerations and Fluoroscopy in Percutaneous fixation of the Pelvis and Acetabulum. *Journal of American Academy of Orthopaedic Surgeons*, 27, 899–908.

16. Routt, M. L., Simonian, P. T., & Grujic, L. (1995). The retrograde medullary superior pubic ramus screw for the treatment of anterior pelvic ring disruptions: A new technique. *Journal of Orthopaedic Trauma*, 9, 35–44.

17. Giannoudis, P. V., Tzioupis, C. C., Pape, H. C., & Roberts, C. S. (2007). Percutaneous fixation of the pelvic ring: An update. *Journal of Bone and Joint Surgery. British Volume*, 89(2), 145–154.

18. Starr, A. J., Nakatani, T., Reinert, C. M., et al. (2008). Superior pubic ramus fractures fixed with percutaneous screws: What predicts fixation failure?[J]. *Journal of Orthopaedic Trauma*, 22(2), 81–87.

19. Frank, M., Dedek, T., Trlica, J., & Folvarský, J. (2010). Percutaneous fixation of anterior column acetabular fractures–first experience. *Acta Chir Orthop Traumatol Cech*, 77, 99–104.

20. Lu, H., Zhang, Q., Ding, F., Liu, R., & Wu, Q. (2022). Finite Element Analysis of Unilateral versus Bipedicular Bone-Filling Mesh Container for the Management of Osteoporotic Compression Fractures. Biomed Res Int. ; 2022: 6850089.

21. Lu, H., Peng, H., Peng, Z., Liu, D., Wu, Q., & Liu, R. (2021). The Application of Digital Design Combined with 3D Printing Technology in Skin Flap Transplantation for Fingertip Defects during the COVID-19 Epidemic. Biomed Res Int. ; 2021: 5554500.

22. Zhao, Y., Zhang, S., Sun, T., Wang, D., Lian, W., Tan, J., Zou, D., & Zhao, Y. (2013). Mechanical comparison between lengthened and short sacroiliac screws in sacral fracture fixation: A finite element analysis. *Orthopaedics & Traumatology, Surgery & Research : Otsr*, 99, 601–606.

23. Dalstra, M., & Huiskes, R. (1995). Load transfer across the pelvic bone. *Journal of Biomechanics*, 28, 715–724.

24. Phillips, A. T., Pankaj, P., Howie, C. R., Usmani, A. S., & Simpson, A. H. (2007). Finite element modelling of the pelvis: Inclusion of muscular and ligamentous boundary conditions. *Medical Engineering & Physics*, 29, 739–748.

25. Zheng, N., Watson, L. G., & Yong-Hing, K. (1997). Biomechanical modelling of the human sacroiliac joint. *Medical & Biological Engineering & Computing*, 35, 77–82.

26. Zhong, Z., Tong, K., Xie, X., Cao, S., Wang, Q., Zhong, C., & Wang, G. (2018). Finite element analysis of different internal fixation methods for acetabular T-shaped fractures. *Chinese Journal of Orthopaedic Trauma*, 20, 515–522.

27. Pan, C., Liu, X., Cai, X., Wang, Z., & Dong, P. (2015). Three-dimensional finite element analysis of miniplate combined with reconstruction plate internal fixation for posterior acetabular fractures. *Orthopedic Journal of China*, 23, 160–164.

28. Murphy, W. S., Yun, H. H., Hayden, B., et al. (2018). The Safe Zone Range for Cup Anteversion is narrower Than for Inclination in THA.[J]. *Clinical Orthopaedics and Related Research*, 476(2), 325–335.

29. Ochs, B. G., Stuby, F. M., Stoeckle, U., et al. (2015). *Virtual mapping of 260 three-dimensional hemipelvises to analyse gender-specific differences in minimally invasive retrograde lag screw placement in the posterior acetabular column using the anterior pelvic and midsagittal plane as reference[* (Vol. 16, p. 240). J].BMC Musculoskelet Disord.

30. Wang, Q., Zhang, Y., Pan, J., Peng, A., Wu, X., Wang, P., Li, H., Zhang, S., Liu, X., & Zhao, L. (2005). Applied anatomy of retrograde lag screw internal fixation in the superior ramus of pubis. *Chinese Journal of Clinical Anatomy*, 23, 617–619.

31. Suzuki, T., Soma, K., Shindo, M., Minehara, H., & Itoman, M. (2008). Anatomic study for pubic medullary screw insertion. *J Orthop Surg (Hong Kong)*, 16, 321–325.

32. Guo, H. Z., Tang, Y. C., Guo, D. Q., Liang, D., & Zhang, S. C. (2020). Biomechanical evaluation of four different posterior instrumentation techniques for single-level transforaminal lumbar interbody fusion: A finite element analysis. *Am J Transl Res*, 12, 6160–6169.